SCIENCE CHINA
Chemistry

• ARTICLES •
• SPECIAL TOPIC • The Frontiers of Chemical Biology and Synthesis

January 2012 Vol.55 No.1: 118–124
doi: 10.1007/s11426-011-4446-0

Preparation of true solutions of monomeric amyloidogenic protein/peptide: A critical prerequisite for aggregation kinetic study

DIAO Shu[1†], ZHAO Hong[1†], WANG WeiMao[1] & WU Chi[1,2*]

[1]*Department of Chemistry, The Chinese University of Hong Kong, Hong Kong, China*
[2]*The Hefei National Laboratory of Physical Science at Microscale; Department of Chemical physics, The University of Science and Technology of China, Hefei 230022, China*

Received September 17, 2011; accepted October 22, 2011; published online November 29, 2011

Our dynamic laser light scattering (LLS) study shows that the current widely used protocols of dissolving amyloidogenic protein/peptide do not really result in a true solution; namely, there always exist a trace amount of interchain aggregates, which greatly affect the association kinetics, partially explaining why different kinetics were reported even for a solution with identical protein and solvent. Recently, using a combination of the conventional dissolution procedure and our newly developed ultra-filtration method, we have developed a novel protocol to prepare a true solution of amyloidogenic protein/peptide without any interchain aggregates. The resultant solutions remain in their monomeric state for at least one week, which is vitally important for further study of the very initial stage of the interchain association under the physiological conditions because more and more evidence suggests that it is those small oligomers rather than large fabric aggregates that are cytotoxic. In addition, this study shows that combining static and dynamic LLS can lead to more physical and microscopic information about the protein association instead of only the size distribution.

amyloidogenic protein/peptide, laser light scattering, monomer, ultra-filtration

1 Introduction

Misfolding and aggregation of amyloidogenic protein/peptide are frequently found in β-sheet-rich fibrillar protein conformation known as amyloid, which is thought to be involved in the onset of neurodegenerative diseases, ranging from Alzheimer and polyglutamine (polyQ) diseases to transmissible spongiform encephalopathies [1, 2]. While amyloid deposits are hallmarks of many neurodegenerative diseases, the mechanism by which these proteins/peptides gain their neurotoxic function upon misfolding and aggregation remains unclear. In the past forty years, amyloid deposits have been thought as causative agents in the degenerative process.

Recently, some experimental evidence suggested that a group of still poorly defined oligomers, rather than the amyloid deposits themselves, are the true toxic conformations [3, 4]. These results highlight the importance of studying the very initial stage of the aggregation process. To gain insight into this initial oligomer formation stage, one must start with a solution that contains only individual (monomeric) protein/peptide chains. Otherwise, the kinetic study would be compromised. For example, previous studies have revealed that the protein aggregation follows a nucleation-and-elongation mechanism with a significant induction lag time, but dramatically different aggregation kinetics were generated by different laboratories even for an identical starting protein/peptide; namely, this induction lag time

*Corresponding author (email: chiwu@cuhk.edu.hk)
†Contributed equally to this work.

varied from minutes to days [5–7]. In our point of view, such a huge discrepancy could be due to the presence of variable trace amounts of oligomer seeds with different sizes in the initial protein/peptide solutions that serve as the template for further aggregation. On the other hand, Giuffrida *et al*. showed that different from neurotoxic native β-amyloid 1-42 ($A\beta_{1\text{-}42}$, pathogenic factor in Alzheimer's disease) dimers and oligomers, monomeric $A\beta_{1\text{-}42}$ are devoid of neurotoxicity and may even act to support neuronal survival [8]. These studies clearly demonstrate how vitally important to start with the well-defined monomeric state when we try to study the association kinetics of amyloidogenic protein/peptide in solutions.

Since amyloidogenic protein chains have a strong tendency to aggregate in an aqueous solution, it has always been a challenge to reliably characterize and monitor the aggregation process. Various methods have been claimed, established and used in practice to dissolve biologically synthesized amyloidogenic proteins or chemically synthesized amyloidogenic peptides into individual chains in aqueous solution before initiating the aggregation process. Georgalis *et al*. added a Glutathione S-transferase tag (GST-tag) to Huntington exon1 protein in order to increase its solubility and prevent its aggregation during the processes of expression and purification. In this way, the chain aggregation was initiated by using a site-specific protease to cleave off the GST-tag [9]. Chen *et al*. used another approach to disaggregate chemically synthesized polyQ peptides in order to study the aggregation in a reproducible and quantitative fashion. Namely, they first treated the peptide chains with volume ratio 1:1 Trifluoroacetic acid/Hexafluoroisopropanol (TFA/HFIP), then dissolved them in water at pH 3, and finally initiate the aggregation process by adjusting pH to 7.5 [10]. Denaturing solvents have also been frequently used to treat amyloidogenic protein/peptide. Lindquist *et al*. applied 8 M guanidine hydrochloride (GdmHCl) to dissolve the biologically synthesized Yeast prion protein Sup35-NM and assumed that it was dissolved into its monomeric state [11].

There is no denying that researchers in this field have done some significant work to explore the aggregation mechanism of amyloidogenic proteins, however, in most of previous studies, the initial dissolution state of amyloidogenic proteins/peptides was characterized mainly by Fourier transform infrared (FTIR), circular dichroism (CD) and fluorescence spectroscopy, which provide conformational information rather than the specific size change. To confirm one has obtained the real monomeric state, size information is indispensable as the direct evidence which can be accurately measured by laser light scattering (LLS) especially at small angle (e.g. 20°). Recently by using this technique to characterize the amyloidogenic proteins/peptides (Huntington exon1 protein, Yeast prion protein Sup35-NM and $A\beta_{1\text{-}42}$) treated by the previously established protocols, we found that although majority of the protein molecules existed as individual chains after following previously established procedures, the solution still contained a trace amount of small particles, presumably the aggregates of a limited number of chains, which hindered our intended study of the very initial stage of the aggregation. To overcome such an obstacle, we have developed a modified protocol to obtain the true monomeric state of amyloidogenic protein/peptide in aqueous solutions. In this paper, we would like to describe our method that should be applicable to other proteins and peptides and show how to combine static and dynamic LLS for accurate characterization of amyloidogenic protein/peptide in aqueous solutions.

In the current study, the biologically synthesized Huntington exon1 protein, Yeast prion protein Sup35-NM and chemically synthesized $A\beta_{1\text{-}42}$ were prepared. The Huntington exon1 gene encoded protein is characterized by glutamine residues with different lengths, ranging from smaller than 36 (wild-type polyQ) to larger than 40 (pathological polyQ, accounted for the onset of Huntington disease) [12, 13]. Two Huntington proteins (polyQ length = 22 and 40, denoted as HD22Q and HD40Q) were respectively selected as typical representatives of the wild and pathological types. The Sup35 protein is a Yeast (*Saccharomyces cerevisiae*) prion protein, a translation termination factor that can convert into insoluble amyloid fibril. The structure of Sup35 protein can be divided into three regions, namely, N, M, and C based on their positions and different functions. Being the prion-determining region, Sup35-NM has been widely accepted as a model to study the amyloidogenic proteins [14]. We also used the 42-amino acid-long peptide $A\beta_{1\text{-}42}$, presumably playing a central and vital role in the pathogenesis of Alzheimer's disease [15], to test whether our protocol is also applicable to smaller amyloidogenic peptides.

2 Results and discussion

2.1 Huntington exon1 protein

In order to obtain the water-soluble Huntington exon1 protein, we first followed the GST-tag method [9], presumably that the GST tag is able to increase the solubility of the fused Huntington protein and provide steric hindrance to each protein molecule, lowering the chance of collision and aggregation. However, dynamic LLS analysis revealed that even for the freshly purified GST-tagged fusion HD22Q, there clearly existed a peak located at ~60 nm in the intensity-weighted hydrodynamic radius distribution, $f(R_h)$, (SI Figure 1), indicating some inter-chain aggregation, suggesting GST alone is not sufficient to keep Huntington exon1 protein in monomeric state even for HD22Q, not to mention the others with longer polyQ.

However, eq. (1) (in methods section) shows that at a sufficiently low angle and low concentration, $[R_{vv}(q = 0)/KC] = M_w$, where $C = W/V$, a mass concentration (g mL^{-1}), and M_w is defined as $(\Sigma W_i M_i)/W$. Therefore, $\langle I_s(q=0)\rangle \propto$

$\sum W_i M_i = \sum n_i M_i^2$ with n_i and M_i being the number and molar mass of the *i*th scattering object, respectively. It shows that one 100-nm particle scatters 10^6 times of light than one 10-nm particle if we assume that the particles are uniform because $M_i \propto R_i^3$. In other words, one interchain aggregate with the size of 100 nm is equivalent to 10^6 individual chains in the intensity-weighted distribution. Therefore, the large peak located at ~60 nm only represents a very small number of the interchain aggregates.

In order to prepare a solution without any interchain aggregates, we then followed a widely adopted TFA/HFIP treatment protocol, originally developed for synthetic polyQ peptides [10], to see whether it can dissolve Huntington exon1 proteins into individual chains in aqueous solutions. Figure 1(a) clearly showed that even after the 1:1 TFA/HFIP treatment, the solutions still contained some interchain aggregates. A comparison of the two treated proteins revealed that for HD22Q much more Huntington protein chains were in their monomeric state with an average hydrodynamic radius (R_h) around 3 nm. However, for HD40Q, there were more interchain aggregates in the solution, which is understandable because of the longer polyQ segment. Although the number of interchain aggregates was actually small, they were clearly not negligible, especially when we focus on the initial stage of aggregation kinetics. Moreover, they could serve as "seeds" for further chain stacking and fiber elongation. Nevertheless, Figure 1(a) showed that the TFA/HFIP treatment method alone was not sufficient to completely remove the interchain aggregates in the solution even though people have assumed it in some previous kinetic studies.

In order to prepare a true solution of the Huntington protein without any interchain aggregates, we modified the aforementioned protocol on the basis of our previous finding in the studies of ultra-filtration of polymer chains through a 20-nm nanopore under an elongation flow [16]. Namely, linear chains can pass through the nanopore when the flow rate reaches a critical value, independent of the chain length, but not the interchain aggregates, particles and polymer chains with other topologies [17, 18]. Our current ultra-filtration setup essentially includes a gastight syringe (SEG), a syringe pump (Harvard PHD 2000) and a membrane filter (Whatman anotop 10). The membrane filter has a double layer structure. The upper layer is 59-μm thick with billions of 200-nm pores; while the lower layer is only 1-μm thick with smaller 20-nm pores (Supplementary Figure 2). Each of the smaller pore is covered by a larger 200-nm pore. The pore density is ~5 × 10^8 cm^{-2}. It should be noted that the 20-nm membrane filter which has uniform pore size is crucial for obtaining the real monomers. In practice, a 100-kDa molecular mass cutoff filter (eg. Ultrafree-MC, Millipore) is more frequently used to remove the small aggregates [19, 20], however, this kind of membrane has an obviously different structure from the membrane we used. It has a 3-dimentional network structure with no uniform orientation and pore size of which the matrix void spaces vary in their degree of complexity or tortuosity. In our opinion, such kind of membrane filter is incompetent for obtaining a true monomeric protein solution since small aggregates/oligomers have a chance to pass through the membrane due to the nonuniform of the pores.

Figure 1(b) shows two typical intensity-weighted R_h distribution of HD22Q and HD40Q in pH 3 water adjusted by TFA after the ultra-filtration, where the flow rate of 1 mL h^{-1} was chosen to push individual protein chains through the membrane filter but not the interchain aggre-

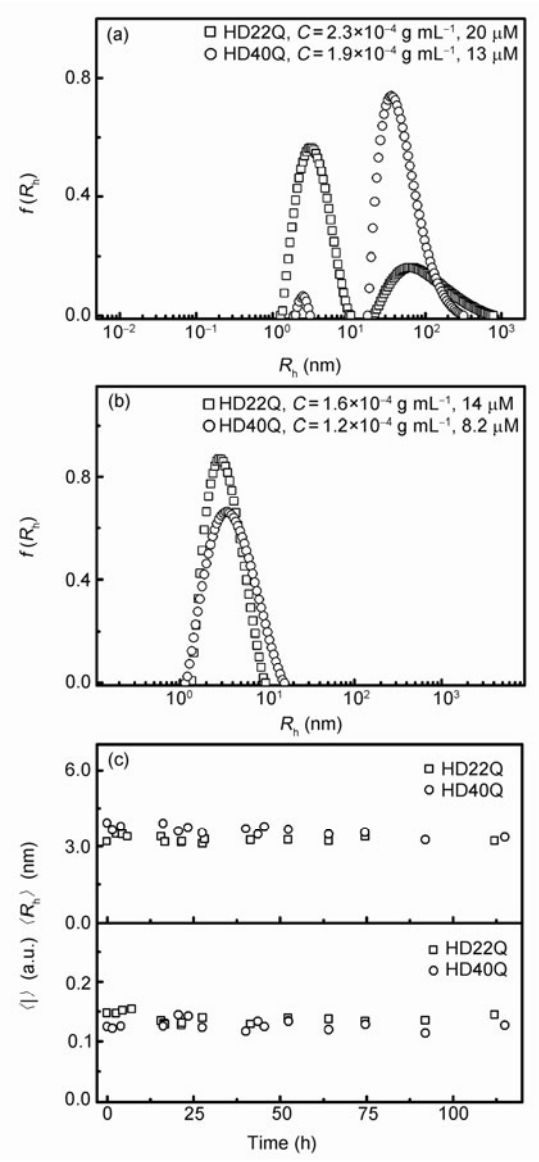

Figure 1 (a) Intensity-weighted R_h distributions of two Huntington exon1 proteins in aqueous solutions at pH 3, after treatment with TFA/HFIP protocol; (b) intensity-weighted R_h distributions of HD22Q and HD40Q proteins, respectively, in aqueous solution (pH 3, adjusted with TFA) after TFA/HFIP treatment and ultra-filtration; (c) time dependent average R_h and average scattering light intensity (<*I*>) of HD22Q and HD40Q in pH 3 water (adjusted with TFA) during 5 days.

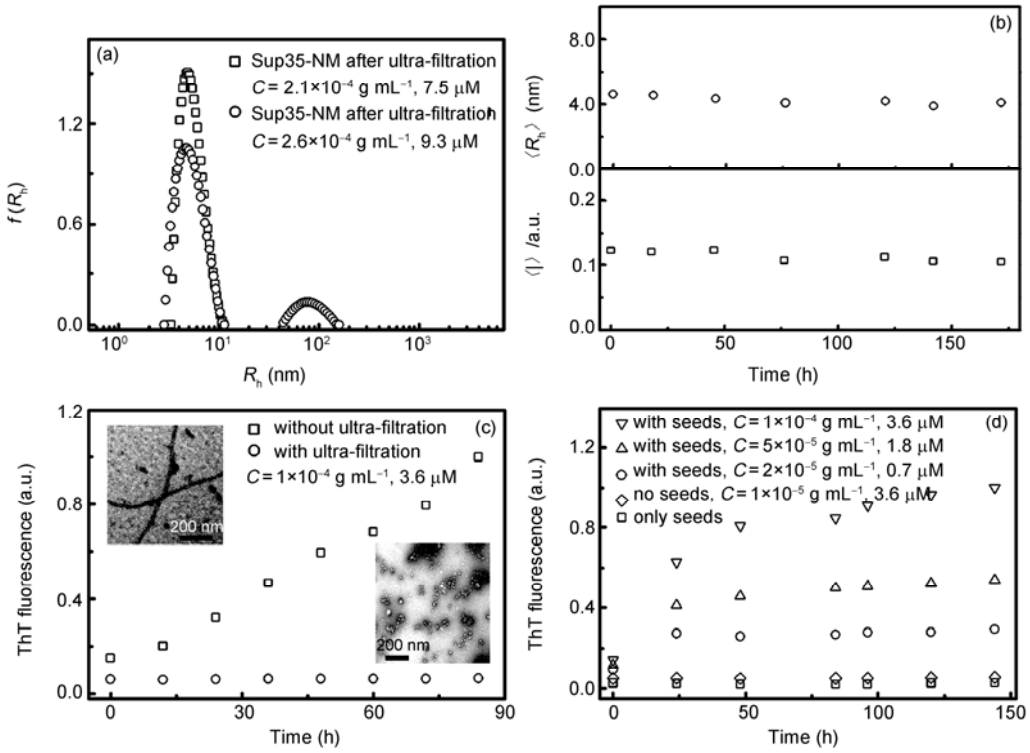

Figure 2 (a) Intensity-weighted R_h distributions of Sup35-NM protein in 8 M GdmHCl (pH 7.4) before and after ultra-filtration; (b) time dependent R_h and scattering light (<*I*>) intensity of Sup35-NM protein in 8 M GdmHCl (pH 7.4); (c) time dependent ThT fluorescence intensity of two Sup35-NM solutions in PBS (pH 7.4) with and without removal of a trace amount of interchain aggregates, where insets are their corresponding TEM images at t = 84 h; (d) time dependent ThT fluorescence intensity of Sup35-NM solutions with different protein concentrations but a fixed amount of sonicated fabric seeds (5% w/w).

gates. Figure 1(b) clearly shows that the peak on the right in Figure 1(a) disappeared in each case, i.e., the trace amount of the interchain aggregates remained after the TFA/HFIP treatment was completely removed by the ultra-filtration. The peaks in Figure 1(b) represent individual HD22Q and HD40Q chains, respectively, with an average R_h of 3.2 nm and 3.6 nm at pH 3, which were consistent with the expected size of individual protein chains.

We also confirmed that each peak in Figure 1(b) represents individual protein chains by using static LLS to characterize the weight-averaged molar mass (M_w) of the Huntington protein after the TFA/HFIP and ultra-filtration treatments in the angular range 20°–120° with step 1°. First, we measured the value of refractive index increment (dn/dC), a required parameter in the determination of M_w on the basis of eq. (1) (in Methods section), by using a novel laser differential refractometer [21] (dn/dC = 0.31 mL g^{-1} for protein in 8 M GdmHCl, dn/dC = 0.28 mL g^{-1} for protein in aqueous solutions at pH 3). We found that after the TFA/HFIP and ultra-filtration treatments, HD22Q and HD40Q in aqueous solutions at pH 3 have M_w of 1.15 × 10^4 g mol^{-1} and 1.39 × 10^4 g mol^{-1}, respectively, fairly close to their corresponding theoretical values of 11,750 g mol^{-1} and 14,105 g mol^{-1}. A combination of static and dynamic LLS measurements enables us to safely conclude that our modified method can lead to a true solution of the biologically synthesized Huntington exon1 proteins, i.e., the proteins exist as individual chains without any interchain aggregation in aqueous solutions at pH 3.

Further, we studied how long HD22Q and HD40Q could exist as individual chains in aqueous solutions at pH 3 by using dynamic LLS to follow their corresponding R_h and the scattering light intensity versus time. Figure 1(c) shows that at pH 3 individual HD22Q and HD40Q chains did not aggregate up to at least 5 days, which lays a foundation for future study of the initial stage of these protein chains under the physiological conditions.

2.2 Sup35-NM protein

Besides organic solvents, denaturing agents have also been frequently applied to "dissolve" amyloidogenic protein/peptide. Lindquist *et al*. tried to use GdmHCl (up to 8 M) to prepare the Yeast prion protein Sup35-NM solution and judged the solution state from its CD spectrum that only indicated that there was no detectable secondary structure inside the solution. To test whether there still exist some interchain aggregates in the Sup35-NM solution, we followed the same protocol used by Lindquist e*t al*. [11] but applied more sensitive and accurate LLS characterization. Figure 2(a) clearly shows that using the protocol, most of Sup35-NM were indeed dissolved into individual chains but

a trace amount of interchain aggregates with an average R_h of ~80 nm still existed in the solution, revealing that this strong denaturant was still not sufficient to completely dissolve Sup35-NM into individual chains to form a true solution of individual chains that were represented by the peak located at ~5 nm.

Figure 2(a) also shows that using the described ultra-filtration method, we could completely remove the trace amount of interchain aggregates, resulting in a true solution of Sup35-NM containing only individual chains with an average R_h of 5.0 nm at pH 7.4, consistent with the expected size of individual protein chains. Further, we used static LLS to characterize such an obtained solution and found that the M_w of Sup35-NM in the solution was 2.80×10^4 g mol^{-1}, fairly close to the theoretical value of 29,120 g mol^{-1}, revealing the obtention of a true solution of the Sup35-NM protein without any interchain aggregates in 8 M GdmHCl, 20 mM Tris at pH 7.4. We also investigated the stability of such a solution. Figure 2(b) showed that in 8 M GdmHCl, individual Sup35-NM chains could remain in their monomeric state for up to one week.

Once after obtaining the true solution of Sup35-NM without interference of the interchain aggregates, we did some preliminary kinetic studies of the interchain association under the physiological condition (PBS, pH 7.4) by using the classical Thioflavin T (ThT) fluorescence assay [22]. Not surprisingly, the protein treated with our modified protocol behaved quite differently from the protein treated with conventional method, i.e., with no ultra-filtration treatment.

Figure 2(c) shows the ThT fluorescence intensity of the Sup35-NM solution clarified with the ultra-filtration method, i.e., with no interchain aggregates, nearly remained a constant even after 90 h, while that of the Sup35-NM solution prepared by the conventional protocol without the removal of the trace amount of the interchain aggregates increased with time, clearly indicating the formation of the β sheet-rich structures, which were confirmed by their morphological differences (small amorphous structure versus large amyloid-like fibers), as shown in the insets of Figure 2(c) (images from transmission electron microscope, TEM). Such a huge discrepancy is presumably because the trace amount of small aggregates in the conventionally prepared protein solution could serve as template (seeds) for further aggregation and fiber elongation. Our results might partially explain why some dramatically different aggregation kinetics were previously reported even for a solution of an identical protein and solvent.

Further, we tested whether Sup35-NM prion in the solution after the ultra-filtration is still active by using the seeding assay [23]. The seeds were prepared by briefly sonicating preformed Sup35-NM fibers with a probe sonicator at 50 watt for 15 s. The seeds should be freshly prepared before use. Figure 2(d) shows that for a given amount of the seeds (5% w/w), the ThT fluorescence intensity increased with the monomer concentration, indicating the remaining prion activity. The current results also clearly reveal that it is vitally important in a kinetic study to start with a true solution of amyloidogenic proteins/peptides without interchain aggregates.

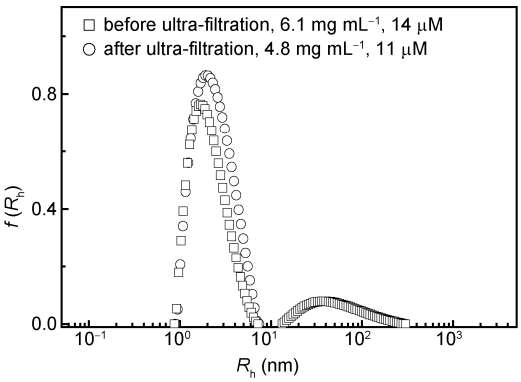

Figure 3 Intensity-weighted R_h distributions of $A\beta_{1-42}$ in aqueous solution (pH 3, adjusted with TFA) before and after ultra-filtration.

2.3 $A\beta_{1-42}$

$A\beta_{1-42}$ was synthesized to test whether our modified protocol was applicable to smaller amyloidogenic peptides. Chemically synthesized $A\beta_{1-42}$ was treated according to the same protocol for the Huntington protein. Figure 3 showed that using the ultra-filtration we were able to completely remove small oligomers. The $A\beta_{1-42}$ chains in the resultant solution had an average R_h of ~1.5 nm and a M_w of 4.3×10^3 g mol^{-1}, respectively, characterized by dynamic and static LLS. Both $<R_h>$ and M_w were close to their corresponding expected theoretical values (4514 g mol^{-1}) of individual $A\beta_{1-42}$ chains, confirming that $A\beta_{1-42}$ in the clarified solution existed as individual chains with no interchain aggregates.

In summary, a modified protocol of combining the conventional method and ultra-filtration has been established. Using this protocol, we are able to prepare a true solution of amyloidogenic protein/peptide with no interchain aggregate. Unlike in the conventional protocol, amyloidogenic protein/peptide chains in the true solution remain stable and as individual chains for at least one week, which lays a solid foundation for further study of the interchain association kinetics under the physiological conditions, presumably because of the removal of the trace amount of oligomers that act as seeds to induce further interchain association and fiber formation/growth. Our current results demonstrate that it is vitally important to start with a pure solution if one tries to study the kinetics of the protein aggregation, especially when the focus is on the initial stage, because the existence of a trace amount of oligomers in the initial protein solution can greatly influence the aggregation process and tarnish the experimental results. Finally, we also like to emphasize that it is important to combine static and dynamic laser light

scattering in the study of protein solutions because it will give us more microscopic parameters.

3 Methods

3.1 TFA/HFIP treatment

$A\beta_{1\text{-}42}$ and freshly purified HD22Q/40Q were respectively desalted using ultrafiltration device (Millipore) followed by freeze-drying; a solvent mixture of 1:1 (*V*/*V*) TFA/HFIP was then added to dissolve each lyophilized protein powder overnight. The sample was further air-dried by an argon gas stream and then by vacuum to completely remove TFA and HFIP. The deionized water at pH 3 (adjusted with TFA) was added to make a solution under votexing. Possible residual aggregates were removed by centrifugation at 30,000 *g* for 30 min. The top two-thirds of the solution was used for laser light scattering analysis.

3.2 Protein/peptide preparation

Expression of Sup35-NM and Huntington exon1 protein were performed using the *E. coli* BL21 (DE3) and LB medium supplemented with 50 μg mL^{-1} kanamycin and 100 μg mL^{-1} ampicillin respectively. Protein expression was induced with 1 mM IPTG when cell culture reached an OD_{600} value of 0.4. Both proteins were purified with the HisTrap HP column (GE Healthcare). $A\beta_{1\text{-}42}$ was synthesized according to the described method by using the ChemMatrix resin [24]. The standard Fmoc chemistry was applied. The 15-min deprotection was followed by 35-min coupling for each amino acid. The peptide was then cleaved by Reagent K (82.5% TFA:5% phenol:5% H_2O:5% thioanisole:2.5%) to minimize the side reactions and precipitated by cold ether before the lyophylization.

3.3 Laser light scattering

A commercial LLS spectrometer (ALV/DLS/SLS-5022F) equipped with a multi-τ digital time correlator (ALV5000) and a cylindrical 22-mW He-Ne laser (632.8 nm, Uniphase) as the light source was utilized to characterize the treated proteins. In static LLS, the weight-average molar mass, M_w, the z-average root-mean-square radius of gyration, $\langle R_g^2 \rangle^{1/2}$, and the second virial coefficient, A_2, of scattering objects in dilute solutions can be determined from the angular dependence of the excess absolute scattering intensity, known as the Rayleigh ratio $R_{vv}(q)$, according to

$$\frac{KC}{R_{vv}(q)} \approx \frac{1}{M_w}\left(1+\frac{1}{3}\left\langle R_g^2\right\rangle q^2\right)+2A_2C \quad (1)$$

where $K = 4\pi^2 n^2 (dn/dC)^2/(N_A \lambda_0^4)$, and $q = (4\pi n/\lambda_0)\sin(\theta/2)$ with N_A, n, θ, and λ_0 being the Avogadro number, the solution refractive index, the scattering angle, and the wavelength of the light in vacuum, respectively; and C is the protein concentration.

In dynamic LLS, the Laplace inversion of each measured intensity–intensity time correlation function, $G^{(2)}(t,q)$, in the self-beating mode gives a line-width distribution, $G(\Gamma)$. For a pure diffusive relaxation, Γ is related to the translational diffusion coefficient D by $\Gamma = Dq^2$ when $q \to 0$ and $C \to 0$. D is further related to the hydrodynamic radius R_h by the Stokes-Einstein equation, $R_h = k_B T/(6\pi\eta D)$, where k_B, T, and η are the Boltzmann constant, the absolute temperature, and the viscosity, respectively. The scattering angle used in dynamic LLS in this study was 20°. All of the LLS experiments were performed at 25 °C.

3.4 Ultra-filtration

As described in the main text.

3.5 Thioflavin T fluorescence assay

The ThT assay was carried out as described [20]. Sup35NM monomer sample in 8 M GdmHCl, 5–10 mg mL^{-1} (as requirement), was 100-fold diluted with PBS pH 7.4 to eliminate the influence of GdmHCl for ThT assay. The dilution would induce the aggregation. ThT fluorescence was monitored using a fluorescence spectrophotometer (HITACHI F-7000) with excitation at 450 nm and emission at 490 nm.

3.6 Transmission electron microscopy

For each sample, 10 μL protein solution was placed on a carbon-coated copper grid, absorbed for 1 min, and the excess sample was removed with filter-paper. The sample was stained with 10 μL 1% (w/v) uranyl acetate for 1 min and blotted. The copper grid was washed with 10 μL deionized water. All samples were imaged by using an FEI CM120 microscope operated at 120 kV.

3.7 Protein concentration determination

Standard BCA assay, Bradford assay and UV absorbance measurement at 280 nm have been applied for protein quantitation. Concentration data were collected after ultrafiltration in case the eliminated small aggregates bias the measurement.

We thank Prof. Edwin Ho-Yin CHAN for gifting the Huntington exon1 gene plasmids and Prof. Jiang XIA for assistance in Aβ1-42 peptide synthesis. The financial support of the National Natural Science Foundation of China Project (20934005) and the Hong Kong Special Administration Region Earmarked Project (CUHK4046/08P, 2160365; CUHK4039/08P, 2160361; CUHK4042/09P, 2160396) are gratefully acknowledged.

1 Selkoe DJ. Folding proteins in fatal ways. *Nature*, 2003, 426: 900–904

2 Chiti F, Dobson CM. Protein misfolding, functional amyloid, and human disease. *Annu Rev Biochem*, 2006, 75: 333–366
3 Kayed R, Head E, Thompson JL, McIntire TM, Milton SC, Cotman CW, Glabe CG. Common structure of soluble amyloid oligomers implies common mechanism of pathogenesis. *Science*, 2003, 300: 486–489
4 Shankar GM, Li S, Mehta TH, Garcia-Munoz A, Shepardson NE, Smith I, Brett FM, Farrell MA, Rowan MJ, Lemere CA, Regan CM, Walsh DM, Sabatini BL, Selkoe DJ. Amyloid-beta protein dimers isolated directly from Alzheimer's brains impair synaptic plasticity and memory. *Nat Med*, 2008, 14: 837–842
5 Palhano FL, Rocha CB, Bernardino A, Weissmuller G, Masuda CA, Montero-Lomelí M, Gomes AM, Chien P, Fernandes PM, Foguel DA. fluorescent mutant of the NM domain of the yeast prion Sup35 provides insight into fibril formation and stability. *Biochemistry*, 2009, 48: 6811–6823
6 Glover JR, Kowal AS, Schirmer EC, Patino MM, Liu JJ, Lindquist S. Self-seeded fibers formed by Sup35, the protein determinant of [PSI+], a heritable prion-like factor of *S. cerevisiae. Cell*, 1997, 89: 811–819
7 Hess S, Lindquist SL, Scheibel T. Alternative assembly pathways of the amyloidogenic yeast prion determinant Sup35-NM. *Embo Reports*, 2007, 8: 1196–1201
8 Giuffrida ML, Caraci F, Pignataro B, Cataldo S, De Bona P, Bruno V, Molinaro G, Pappalardo G, Messina A, Palmigiano A, Garozzo D, Nicoletti F, Rizzarelli E, Copani A. Beta-amyloid monomers are neuroprotective. *J Neurosci*, 2009, 29: 10582–10587
9 Georgalis Y, Starikov EB, Hollenbach B, Lurz R, Scherzinger E, Saenger W, Lehrach H, Wanker EE. Huntingtin aggregation monitored by dynamic light scattering. *Proc Natl Acad Sci USA*, 1998, 95: 6118–6121
10 Chen SM, Wetzel R. Solubilization and disaggregation of polyglutamine peptides. *Protein Sci*, 2001, 10: 887–891
11 Scheibel T, Lindquist SL. The role of conformational flexibility in prion propagation and maintenance for Sup35p. *Nat Struct Biol*, 2001, 8: 958–962
12 Cummings CJ, Zoghbi HY. Trinucleotide repeats: mechanisms and pathophysiology. *Annu Rev Genomics Hum Genet*, 2000, 1: 281–328
13 Walker FO. Huntington's disease. *Lancet*, 2007, 369: 218-228
14 Chen CY, Rojanatavorn K, Clark AC, Shih JC. Characterization and enzymatic degradation of Sup35NM, a yeast prion-like protein. *Protein Sci*, 2005, 14: 2228–2235
15 Walsh DM, Selkoe DJ. A beta oligomers—a decade of discovery. *J Neurochem*, 2007, 101: 1172–1184
16 Chen QJ, Zhao H, Ming T, Wang JF, Wu C. Nanopore extrusion-induced transition from spherical to cylindrical block copolymer micelles. *J Am Chem Soc*, 2009, 131: 16650–16651
17 Ge H, Jin F, Li JF, Wu C. How much force is needed to stretch a coiled chain in solution? *Macromolecules*, 2009, 42: 4400–4402
18 Ge H, Wu C. Separation of linear and star chains by a nanopore. *Macromolecules*, 2010, 43: 8711–8713
19 Foguel D, Palhano FL, Rocha CB, Bernardino A, Weissmuller G, Masuda CA, Montero-Lomeli M, Gomes AM, Chien P, Fernandes PMB. A fluorescent mutant of the NM domain of the yeast prion Sup35 provides insight into fibril formation and stability. *Biochemistry*, 2009, 48: 6811–6823
20 Tanaka M, Ohhashi Y, Ito K, Toyama BH, Weissman JS. Differences in prion strain conformations result from non-native interactions in a nucleus. *Nat Chem Bio*, 2010, 6: 225–230
21 Wu C, Xia KQ. Incorporation of a differential refractometer into a laser light-scattering spectrometer. *Rev Sci Instrum*, 1994, 65: 587–590
22 LeVine H. Quantification of beta-sheet amyloid fibril structures with thioflavin T. In *Amyloid, Prions, and Other Protein Aggregates*. Academic Press Inc, 1999, 309: 274
23 Colby DW, Zhang Q, Wang S, Groth D, Legname G, Riesner D, Prusiner SB. Prion detection by an amyloid seeding assay. *Proc Natl Acad Sci USA*, 2007, 105: 1774–11774
24 Garcia-Martin F, Quintanar-Audelo M, Garcia-Ramos Y, Cruz LJ, Gravel C, Furic R, Côté S, Tulla-Puche J, Albericio F. ChemMatrix, a poly(ethylene glycol)-based support for the solid-phase synthesis of complex peptides. *J Comb Chem*, 2006, 8: 213–220

SCIENCE CHINA
Chemistry

• SUPPORTING INFORMATION •

January 2012 Vol.55 No.1: 1
doi: 10.1007/s11426-011-4446-0

Preparation of true solutions of monomeric amyloidogenic protein/peptide: A critical prerequisite for aggregation kinetic study

DIAO Shu[1†], ZHAO Hong[1†], WANG WeiMao[1] & WU Chi[1,2*]

[1]*Department of Chemistry, The Chinese University of Hong Kong, Hong Kong, China*
[2]*The Hefei National Laboratory of Physical Science at Microscale; Department of Chemical physics, The University of Science and Technology of China, Hefei 230022, China*

Received September 17, 2011; accepted October 22, 2011; published online November 29, 2011

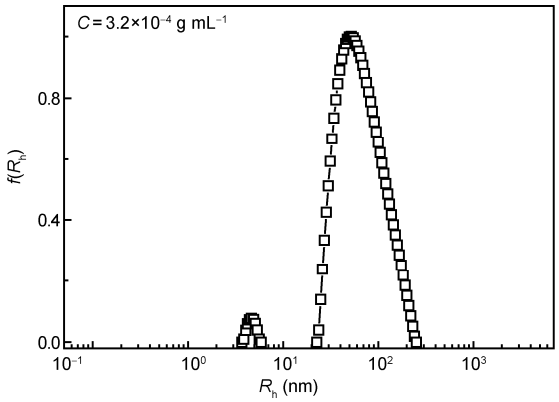

Figure S1 Intensity-weighted hydrodynamic radius distribution of freshly purified GST-HD22Q in PBS (pH 7.4).

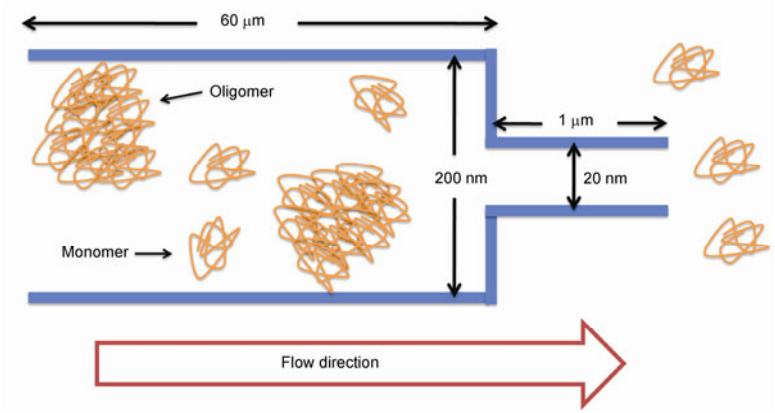

Figure S2 Schematic showing the construction of the filter (Whatman) and the ultra-filtration process.

*Corresponding author (email: chiwu@cuhk.edu.hk)
†Contributed equally to this work.